MEASUREMENT OF HELICOPTER NOISE HEMISPHERES UTILIZING A 100M VERTICAL ARRAY

Marthijn Tuinstra and Pieter Sijtsma
National Aerospace Laboratories (NLR)
Voorsterweg 31, 8316 PR Marknesse
The Netherlands

Abstract

Helicopter noise is composed of several sources of sound that vary in importance, dependent on the emission angle and operating condition. It can generally be sub-divided in noise generated by the main rotor and tail rotor, engine noise and interior noise. An approach to capturing this complex noise pattern is the measurement of noise hemispheres from flight tests.

Trials were held with an Apache AH-64 in order to measure its free space acoustic directivity. The measurement setup consisted of a 100m vertical array containing 93 microphones and a horizontal ground array consisting of 13 microphones. Beamforming was applied to filter out ground reflections for the vertical array microphones by focussing on the helicopter position. A processing algorithm was developed that relies on regression analysis to obtain a model for the acoustic directivity. Directivity functions based on two variable Taylor series and Fourier series were considered. Both approaches yield good results. If a low order approximation is desired, the polynomial fit is better able to capture the measured trend. For a high order approximation, however, the Fourier series fit is better capable to follow rapid changes in directivity.

1. INTRODUCTION

Helicopter noise can be decomposed in several sources of sound. Generally, it can be sub-divided in noise generated by the main rotor and tail rotor, engine noise and interior noise. Characteristic of helicopter noise is that relative importance of each component is strongly dependent on operating conditions and that it possesses a strong directivity.

The accurate prediction of helicopter noise is challenging at the least and therefore a common approach to capturing this complex noise pattern is the measurement of noise hemispheres from flight tests. Trials were held with an Apache AH-64 in order to measure its free space acoustic directivity. The measurement setup consisted of a 100m vertical array containing 93 microphones and a horizontal ground array with 13 microphones. Naturally, the processing into hemispheres brings along its own challenges which will be discussed in this paper.

2. EXPERIMENTAL SETUP

Hemispheres represent the helicopter noise directivity scaled to a certain reference distance R_{ref} for a specific flight condition. The directivity is described in terms of a polar angle ($0 < \theta < \pi$ rad) and lateral angle ($-\pi/2 < \varphi < \pi/2$ rad):
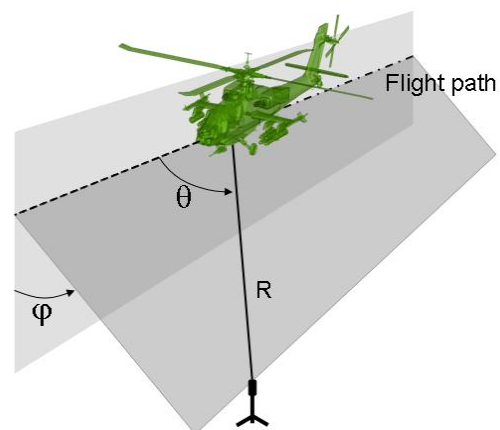

Figure 1 - Coordinate definition

In this an implicit assumption is made that helicopter noise can be described as if it were emitting from a single point in space. The points of departure for hemisphere acquisition were:

- To be able to consider the measured noise to originate from a point source the distance $R >> A$, where A is the size of the helicopter.
- The altitude H should be sufficiently high to stay clear of any influence of the ground surface.
- To minimize measurement inaccuracies (e.g. due to meteorological conditions) R ought to be less than 450m[1].

- The use of ground microphones should be avoided for lateral angles $|\varphi| < 60$ for the same reason[1]. Instead, a vertical array of microphones similar to that used by Brown et al.[2] is desirable.
- Measured signals by microphones in the vertical array are disturbed by reflections of sound via the ground surface. The microphone density in the vertical array shall be sufficient to be able to apply beamforming in order to filter out reflected noise.
- The angular resolution should be as high as possible
- Maximum (ground) velocity of the helicopter is 120kts (61.7m/s)

Considering the above, a vertical array of 200m height and a dense microphone spacing (e.g. ~20cm) would be considered ideal. However, due to practical constraints (cost, availability of microphones, logistics), the height of the vertical array was limited to 96m and contained 93 microphones, with a spacing of 1m in between (4m to 96m). The ground microphones were spaced in a manner that for a level flyover at 85m altitude a $\Delta\varphi$ is obtained of 5°. Figure 2 gives a schematic of the array setup and Figure 3 an impression of the test site.
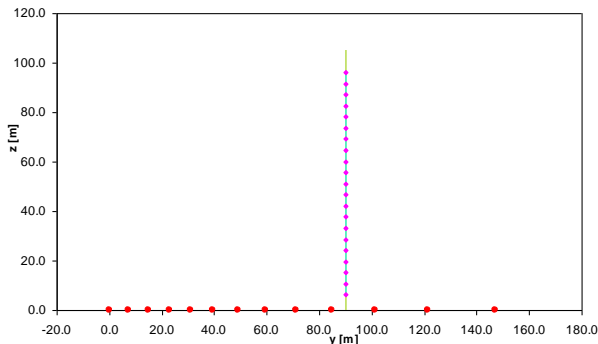

Figure 2 - Side view of the array setup

Three 48-channel GBM Viper frontends were used for data acquisition with LinearX M51 type microphones. The data acquisition rate was 20480Hz.

The helicopter passed by the array at a distance $B = $ 90m at an altitude $H = 85$m. The length of an Apache is approximately $A = 18$m. Then with a distance B = 90m, the angle of sight is approximately 11°. Therefore, when the helicopter is considered as a point source, the polar angle accuracy is in the order of ±5.5°.

Positive and negative lateral angles are obtained by flying pass the array twice, with the array on port side and starboard side respectively. The data acquisition systems were synchronized with GPS time on start of each day of the trials. The helicopter flight track was recorded by GPS to be able to match helicopter position with measured noise.

Figure 3 - Impression of the test site

3. PROCESSING

3.1. Procedure

When carrying out static acoustic tests, for example on a wind tunnel model, it is common practice to reduce measurement uncertainty by means of averaging. This is limitedly possible for moving sources and therefore an alternative procedure is followed:
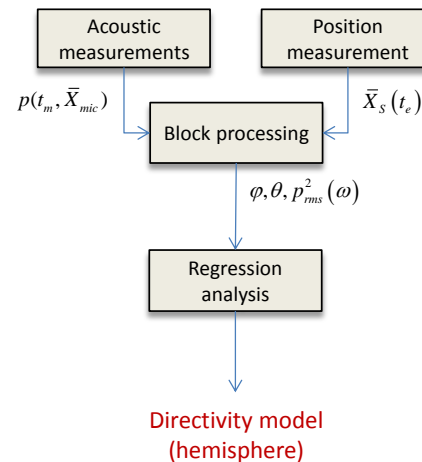

Figure 4 - Schematic of the procedure

The measurement signals are sub-divided into blocks. These blocks are processed into p^2_{rms}, given in the frequency domain, with corresponding emission angles φ and θ. The acoustic pressure is scaled to a reference distance R_{ref}. Based on these parameters a hemisphere model is obtained through regression analysis.

Key points of the above described algorithm are:
- It can be used with unstructured data sets, only requirement is that two variables (θ,φ) and a response (e.g. SPL) are provided
- Repeat measurements can therefore be added effortlessly
- The output is a model, not a table of SPL's
- The degrees of freedom of the model controls how well it follows the original data set (the amount of smoothing)
- It functions as a data compression method

3.2.   Block processing

The measurement signals were sub-divided in blocks of 4096 samples (0.2s, $\Delta f=5Hz$), with an overlap of 50%. Each block was processed using an FFT algorithm with the application of a Hanning window to reduce spectral leakage. The resulting spectra were scaled to a reference distance R_{ref}, taking into account spherical spreading and atmospheric attenuation[3].

To determine the emission angles φ, θ for sound recorded at a time instance t_m the helicopter position at emission time t_e is required. Equation 1 gives the relation between emission time and reception time:

(1) $\qquad t_m = t_e + \left| \overline{X}_S\left(t_e\right) - \overline{X}_{mic} \right| / c$

in which $\overline{X}_S$ and $\overline{X}_{mic}$ are the source and the microphone location respectively; c is the speed of sound. To find the emission time (and related helicopter position) that satisfies relation (1) an iterative root solver was used.

The vertical array microphones were clustered in groups of six microphones. Per cluster a Delay and Sum approach was followed to filter out the effect of ground reflection:

(2) $\qquad p_{cl}\left(\omega\right) = \frac{1}{m} \sum_{n=1}^{m} p_n\left(\omega\right) \frac{R_n}{R_{ref}} e^{i\omega\left(R_n - R_{ref}\right)}$

In this, p_n is the measured complex pressure amplitude, m the number of microphones in a cluster, R_n the distance from the microphone to the source and ω the angular frequency. The polar and lateral angles are defined as the average value over the microphones contained in a cluster. Effects of ground reflections are therefore minimized, yielding high quality data.

From the narrowband spectra 1/3-octave band spectra are derived.

3.3.   Regression analysis

The processing algorithm relies on regression analysis to obtain a model for the acoustic directivity. A two variable regression function, dependent on the lateral angle φ and the polar angle θ, is sought that can adequately describe the emission pattern. For each individual frequency band a directivity function is derived.

Two directivity functions will be examined, an Nth order polynomial (or Taylor series):

(3) $\qquad \Pi_f\left(\varphi,\theta\right) = \sum_{q=0}^{N} \sum_{r=0}^{q} a_{q-r,r}\varphi^{q-r}\theta^r$

and an Nth order truncated Fourier series

(4) $\qquad \Phi_f\left(\varphi,\theta\right) = \sum_{q=-N}^{N} \sum_{r=-N}^{N} a_{q,r} e^{i\left(2\varphi q + 2\left(\theta - \frac{\pi}{2}\right)r\right)}$

The unknown coefficients $a_{q,r}$ and $a_{q-r,r}$ are determined by solving the least squares problem of the overdetermined system of linear equations, provided by the measured emission angles and the related acoustic response in conjunction with equation (3) or (4). The least squares solution is obtained by QR-factorization and subsequently solving a triangular matrix of linear equations. LAPACK and BLAS routines were used.

4.   RESULTS

All results discussed in this section concern a steady level flight at 100kts.

4.1.   Autopower vs. sound pressure level

The acoustic response, used to determine the directivity function, can be defined either in terms of SPL or in terms of p^2_{rms}. In case of static measurements, averaging is based on p^2_{rms}. Therefore, one might argue that it is physically most sound to base the directivity function on acoustic energy (p^2_{rms}) rather than SPL. This has however, an unwanted side effect as is illustrated in the following image:
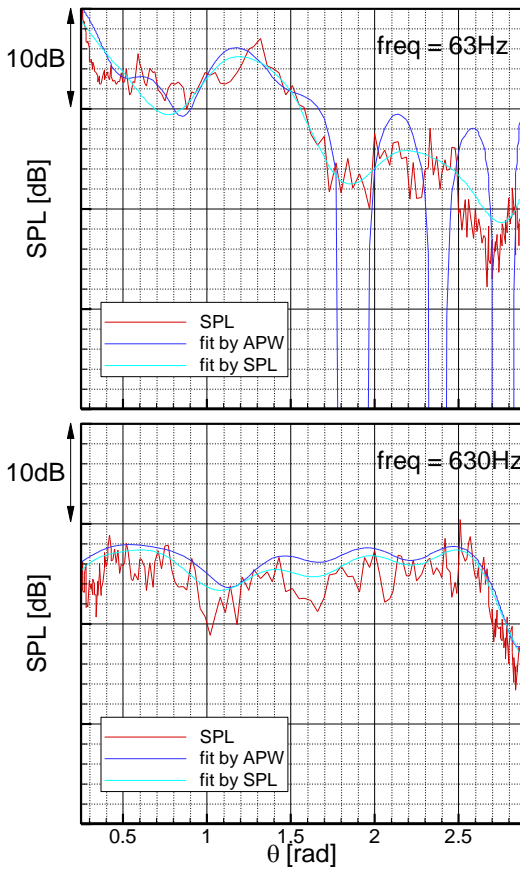
Figure 5 – Measured (red) and model (blue and cyan) 1/3 Octave band levels for a single microphone, scaled to a reference distance R_{ref}, Top: 63Hz band, Bottom: 630Hz band

It is clear that the acoustic energy based model, in particular for the 63Hz band, produces erroneous results. The reason lies in the fact that a least squares projection minimizes the absolute error over the complete hemisphere. Consequently, in case of strong directivity, the local error (or relative error) can become large and even yield negative acoustic energies. It is therefore preferable to use SPL based regression models. These are less biased towards high acoustic levels since the error in the model is minimized with respect to decibels.

Additionally, the impact of averaging based on SPL compared to averaging based on acoustic energy is assessed. First the following definitions are given: SPL_0 is defined as the sound pressure level related to the true average acoustic energy (infinite averaging time). The sound pressure level based on the actual estimate of the average acoustic energy is referred to as SPL_1 (finite averaging time). Lastly, SPL_2 is the sound pressure level that is obtained by direct averaging of SPL.

By Taylor series expansion an approximation of the expected error is derived for finite averaging (expressed in decibels),

(5)

$$E_1 = E\left\{\left(SPL_1 - SPL_0\right)^2\right\}^{\frac{1}{2}} = 4.343 \frac{\sigma_Z}{\overline{p}_{rms}^2 \sqrt{Z}}$$

and averaging based on SPL:

(6)

$$E_2 = E\left\{\left(SPL_2 - SPL_0\right)^2\right\}^{\frac{1}{2}} = 4.343 \frac{\sigma_Z}{\overline{p}_{rms}^2 \sqrt{Z}} \sqrt{1 + \frac{Z}{4}\left(\frac{\sigma_Z}{\overline{p}_{rms}^2}\right)^2}$$

The expectation value of the difference between the two approaches is given by:

(7)

$$E_3 = E\left\{\left(SPL_2 - SPL_1\right)^2\right\}^{\frac{1}{2}} = -E\left\{SPL_2 - SPL_0\right\} = 2.171 \left(\frac{\sigma_Z}{\overline{p}_{rms}^2}\right)^2$$

,which equals to minus the expectation value of $(SPL_2 - SPL_0)$. Direct averaging of SPL therefore tends to underpredict SPL_0. In the above equations E stands for the expectation value, σ_Z the standard deviation, Z the number of averages and $\overline{p}_{rms}^2$ the true average value of p_{rms}^2.

Based on the above equations the magnitude of the errors is assessed. Figure 6 shows the expectation values for E_1, E_2 and E_3 and σ_Z corresponding to $0.12\overline{p}_{rms}^2$, $0.26\overline{p}_{rms}^2$ and $0.52\overline{p}_{rms}^2$. These values are typical for weak (±1dB), medium (±2dB) and strong (±6dB) scatter respectively.
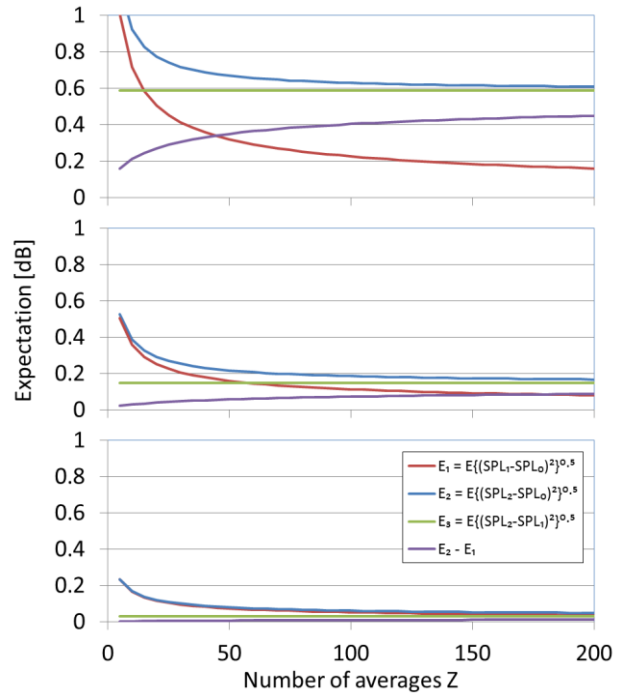

Figure 6 – Expected error values for E1 (red), E2 (blue), E3 (green) and E2-E1 (purple), top: strong scatter, middle: medium scatter, bottom: weak scatter

The figure shows that E_1, as expected, converges to zero for a sufficient number of averages. The required number of averages depends on the data scatter (standard deviation). The expectation value E_2 however, does not converge to zero but to a value given by equation (7). This represents the highest accuracy that can be obtained when SPL based averaging is applied to obtain an estimate of the average acoustic energy. For low and medium scatter the impact can be considered negligible, since this value is sufficiently small (0.03dB and 0.15dB respectively). For strong scatter a maximum accuracy is found of approximately 0.6dB, which is still acceptable, in particular considering that E_1 does not give much better results when the number of averages is not adequate.

Overall it is shown that for a low number of averages the error made in the estimators SPL_1 and SPL_2 is of the same order. For the considered type of measurement the number of averages that can be obtained closely around a point on a hemisphere is limited (<50) as a result of the helicopter movement. Since a hemisphere based on bin-averaged p_{rms}^2 is therefore not expected to yield more accurate results, a regression model based on SPL is justified.

4.2. Beamforming

By clustering the microphones of the vertical array in sub-groups and using a Delay and Sum algorithm, focussed on the helicopter position, contributions to the measured signal by ground reflection can be reduced or filtered out completely. To assess the effectiveness, results for a ground microphone that are uninfluenced by ground reflections, are compared with the vertical array cluster closest to the ground.

Figure 7 shows the 1/3-Octave band spectra for θ equals 80° and 90°. Note that the spectra are obtained from a single block in time of 0.2s and hence no averaging in time has been carried out. The grey lines represent the spectra as are obtained from the individual microphones of the microphone cluster. The cyan line shows the spectrum resulting from application of the Delay and Sum algorithm to the microphone cluster.
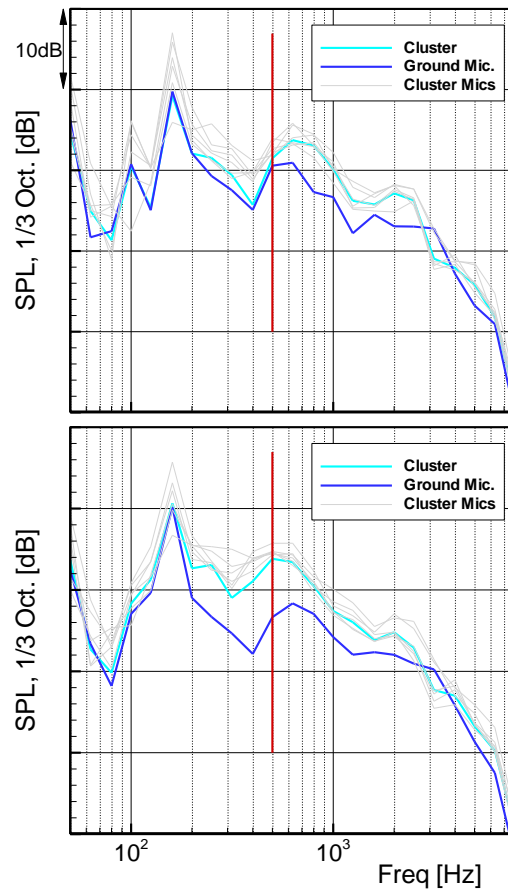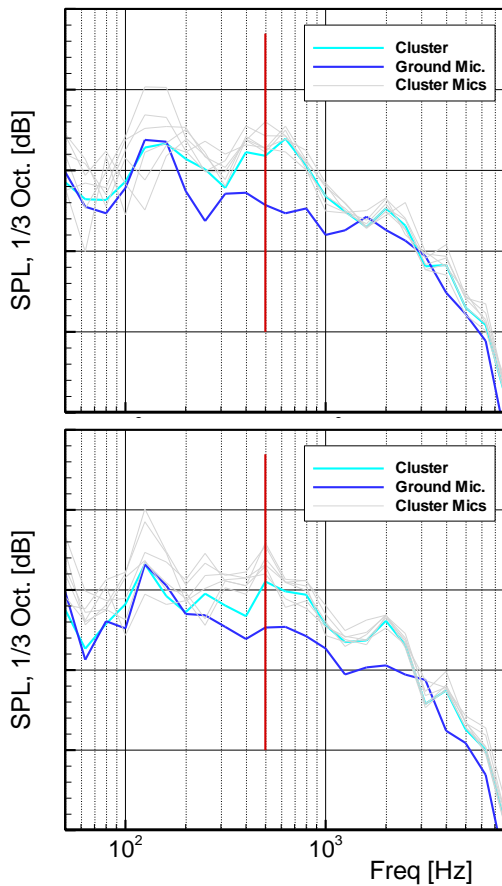

Figure 7 - 1/3 Octave band spectra for the first six array microphones closest to the bottom (grey) , the corresponding Delay and Sum result (cyan) and a ground microphone underneath the array (blue); Top: θ=80° ; Bottom: θ=90°

Beamforming is applied for frequencies up to 500Hz, as indicated by the red line. The distance between microphones is 1m and hence the line array is not suitable for higher frequencies due to expected loss of coherence of the signal. For frequencies up to 200Hz the results compare remarkably well with spectra obtained from the ground microphone (blue lines). Between 200Hz and 500Hz discrepancies are found, however the Delay and Sum result is still closer to that of the ground microphone than what would have been obtained by merely averaging.

Figure 8 additionaly shows the 1/3-Octave band spectra for θ equals 100° and 110°, comfirming the above observations.

Figure 8 - 1/3 Octave band spectra for the first six array microphones closest to the bottom (grey) , the corresponding Delay and Sum result (cyan) and a ground microphone underneath the array (blue); Top: θ=100° ; Bottom: θ=110°

Several aspects contribute to the apparent decrease in effectiveness of the delay and sum algorithm with increasing frequency. Loss of signal coherence over the cluster-array obviously reduces the effectiveness. Another likely candidate however, is the inaccuracy in the helicopter (or source) location data. The GPS system has an intrinsic accuracy which constitutes as a first positioning error. Furthermore, a mismatch in time synchronization with the acoustic acquisition systems can cause an erroneous shift in location that is proportional with velocity (e.g. at 100kts, 0.1s mismatch results in a 5m position error). Lastly, the assumption that the helicopter can be considered as a point source, whilst it is in fact a distributed source also contributes to the position error.

Nonetheless, from the above results it is concluded that the Delay and Sum algorithm is effective in reducing the contribution of ground reflections to the measured signal and hence increases the quality of the noise data.

4.3. Model spectrum

Model spectra are examined and evaluated against measured narrow band spectra.

Figure 9 shows the spectrogram for a ground microphone used in the upcoming evaluation. Note that θ is used instead of time since it is more relevant for the current evaluation.
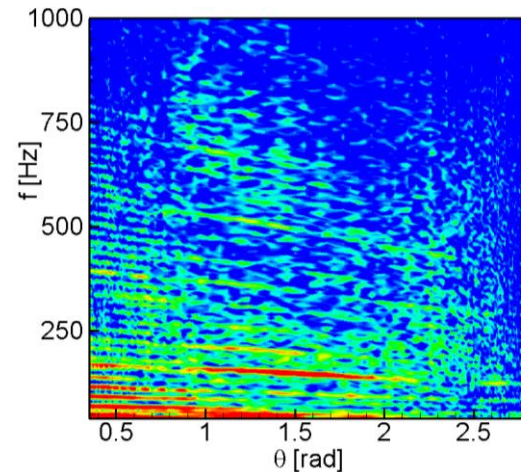

Figure 9 - Spectrogram for a ground microphone

Two observations are made from the above figure. One is that the spectrogram contains multiple tones that are Doppler shifted due to the helicopter's motions. The second observation, although not easily seen, is that data is most densely spaced for small and large polar angles and consequently most sparse around θ=90°. Inspection showed that the data spacing is about 4 times less around θ=90°.

The order N is chosen such that the degrees of freedom of the Fourier model:

$$(6) \qquad DOF_F = 2N^2 + 2N + 1$$

and polynomial model:

$$(7) \qquad DOF_P = N^2/2 + 3/2N + 1$$

are approximately the same to allow direct comparisons. Recall that for each frequency band a regression model is made and no explicit relation exists between frequencies.

Figure 10 shows the measured spectrum (red line) at θ=90° (1.57 rad). The most prominent feature is a tone at 145Hz, which, according to Figure 9 reaches its maximum at θ=90°. Several other tones are visible of which the clearest are at 50Hz, 100Hz and 200Hz. For higher frequencies (>200Hz) they are less prominent and submersed in broadband noise and measurement scatter.
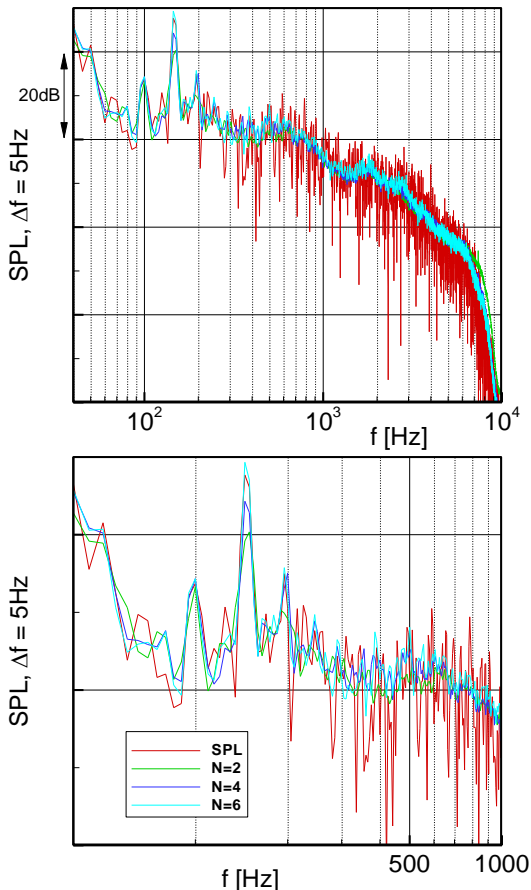
Figure 10 - Measured spectrum at 90 degrees compared to Fourier model for N=2, 4 and 6, Bottom plot is a zoom in on the top plot

Figure 11 - Frequency band SPL as function of polar angle θ, for 100Hz, 145Hz and 1000Hz, origin is shifted for each frequency, for the legend see Figure 10

The model spectra, derived by projecting the measured data on a truncated Fourier series, are shown as well. The green, blue and cyan lines represent respectively a 2nd, 4th and 6th order Fourier model. The lowest order model gives good results for a wide range of frequency bands. When compared with the higher order models it shows the least scatter with frequency. The model output at higher 8kHz and above shows too high levels. At levels 60dB lower than the maximum the relevance is questionable though. The 2nd order model furthermore fails to correctly capture the peak level at 145Hz and 200Hz. It is worthy to note though, that a model based on only 13 empirically determined coefficients is able to capture the directivity described by 40000 responses (nr. of blocks x nr. of microphones) remarkably well.

When the degrees of freedom are increased to 41 (N=4) and 85 (N=6) the model is progressively better able to capture the peak levels at 145Hz and 200Hz. Additional tones (e.g. at 250Hz, 290Hz, 385Hz) become visible that were hidden by scatter in the measured signal. The downside is that the scatter with frequency increases for higher order models. This is easily understood when considering the limiting case of a model for which the degrees of

freedom equal to the number of responses. Since we are no longer dealing with an over determined system, this model is capable to reproduce the measured spectrum exactly.

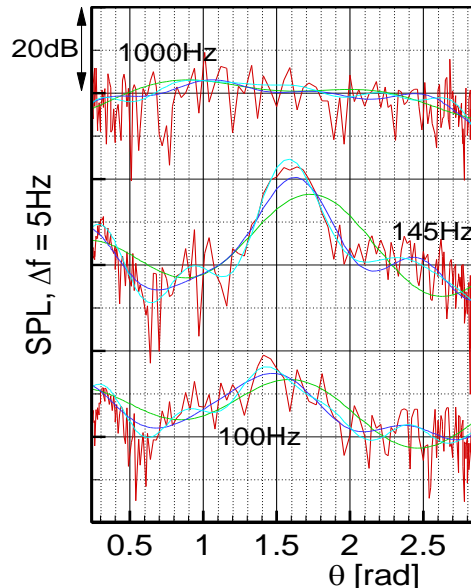In Figure 11 the evolution of SPL with θ of the 100Hz, 145Hz and 1000Hz frequency band is investigated.

The first two bands contain tonal or broadband noise, depending on θ. For example at θ=1.57rad the 145Hz band is crossed by a Doppler shifted tone (Figure 9), causing a 20dB increase compared to the surrounding helicopter broadband noise. This combined with the fact that the data density is sparsest at this polar angle makes it troublesome to capture accurately in the regression models (Note that data density effectively acts as a weighting function for the regression model). The 100Hz band shows a similar image, however the difference of broadband level with tone level is less than at 145Hz. As a result the N=4 model adequately captures the directivity and increasing model order to N=6 yields little benefit. For the 1000Hz band, which contains only broadband noise, all three models nominally provide the same outcome.

In Figure 12 we revisit the spectrum presented in Figure 10. However, in this case polynomial regression models are considered. The green, blue and cyan lines represent a 3nd, 7th and 11th order polynomial model respectively. The order is chosen such that the degrees of freedom are approximately equal to that of the Fourier models. Similar to the Fourier models, the peak at 145Hz is most difficult to capture. Unlike the Fourier models, even the highest order polynomial model is not able to represent the

measured maximum tone level at this frequency correctly. Other tones, in particular higher harmonics, appear less sharp in the model spectra.
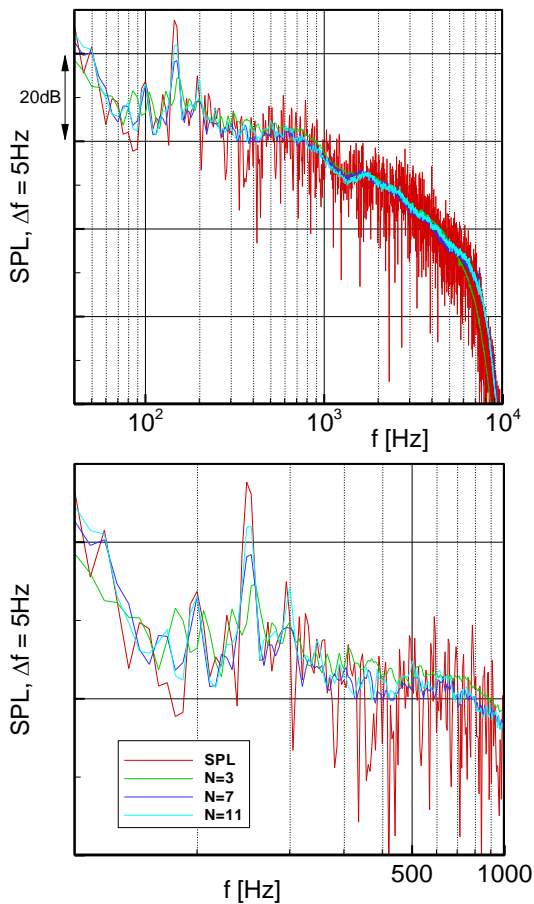

Figure 12 - Measured spectrum at 90 degrees compared to Polynomial model for N=3, 7 and 11, Bottom plot is a zoom in on the top plot

It is observed that the increase in scatter with model order is less than was shown for the Fourier models. In general it can be stated that the polynomial models possess stronger smoothing characteristics than the Fourier models. This statement is confirmed when individual bands are examined (Figure 13). On one hand, data smoothing is considered as a positive property. Data irregularities have less impact on the model as can be seen when comparing with Figure 11. On the other hand, rapid changes in directivity are smoothed as well, as was illustrated by the 145Hz band. This is clearly an unwanted effect.

The introduction of two additional processing measures is expected to significantly improve the results. Firstly, a weighting function could be incorporated in the regression analysis that compensates for the data distribution. This measure is expected to mitigate the model bias towards low and high polar angles. A second measure is to dedopplerize the data before applying the regression analysis. The rapid changes in directivity are mainly caused by Doppler shifted tones moving from one band to another. Dedopplerizing the data would avoid this issue from occurring completely.

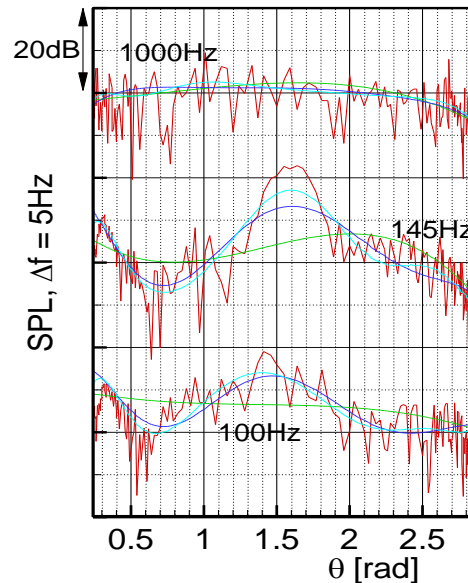Unfortunately the implementation of the above measures was not in the scope of the current work.

Figure 13 - Frequency band SPL as function of polar angle θ, for 100Hz, 145Hz and 1000Hz, origin is shifted for each frequency, for the legend see Figure 12

Both approaches can adequately model the directivity of helicopter noise emission. If a low order model is desired, the polynomial fit is better able to capture the measured trend. When the order of the models is increased however, the Fourier series fit is better capable to follow rapid changes in SPL. This was seen for example at 145Hz, $\theta \approx 90°$.

This section is concluded with the presentation of a typical noise hemisphere:
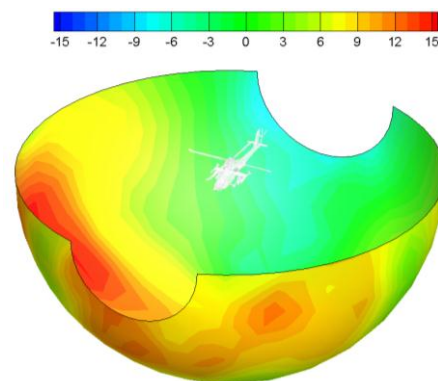

Figure 14 - A typical noise hemisphere based on a N=6 Fourier model

and the modelled version of the spectrogram that was given at the start of this section (Figure 9):
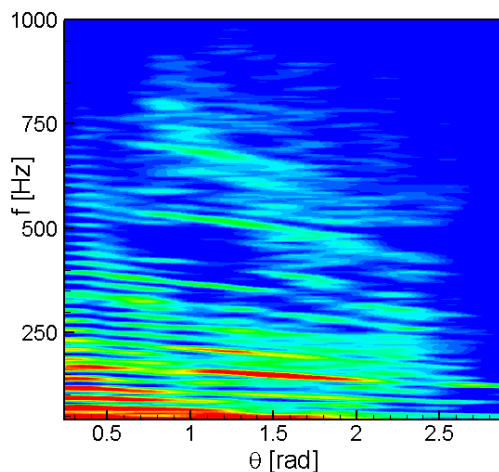
Figure 15 – Modeled spectrogram for a ground microphone, Fourier regression model, N=6

5. CONCLUSIONS

Helicopter noise hemispheres were obtained from measurements utilizing a 100m vertical array in conjunction with a ground array.

A processing method was presented that relies on regression analysis to obtain an empirical model for the helicopter directivity. Two model types were investigated: a truncated Fourier series and a polynomial model. Both types provide good results that match the measurements adequately. The polynomial models possesses the best smoothing characteristics, whereas the Fourier type model is better capable to capture rapid changes in Sound Pressure Level. A beamforming algorithm (Delay and Sum) was implemented and was able to effectively filter out ground reflections at lower frequencies (<500Hz), enhancing data quality of measurements obtained by the vertical array.

Two additional measures were proposed that could further improve processing results. A weighting function could be incorporated in the regression analysis that compensates for the data distribution. Rapid changes in directivity were found to be mainly caused by Doppler shifted tones moving from one band to another. Dedopplerizing the data would avoid this from occurring and consequently the required model order would be reduced.

[1] R.M. Munt; Browne, R.W.; Pidd, M.; Williams, T.; *A measurement and prediction method for determining helicopter noise contours*, 27th European Rotorcraft Forum, Moskou, 11-14 September 2001

[2] R.W. Browne; Munt, R.M.; Simpson, C.R.; Williams, T.; *Prediction of Helicopter Noise Contours for Land Use Planning*, AIAA Paper 2004-2811, Manchester, UK, 2004

[3] H.E. Bass, L C. Sutherland, A.J. Zuckerwar, D.T. Blackstock and D.M. Heste; *Atmospheric absorption of sound: Further developments*, JASA, Vol.97, No.1, pp.680-683, 1995 and erratum in: JASA, Vol.99, No.2, P.1259, 1996